Available online at www.sciencedirect.com
SCIENCE DIRECT®

International Journal of Pharmaceutics 319 (2006) 55–62

INTERNATIONAL JOURNAL OF PHARMACEUTICS

www.elsevier.com/locate/ijpharm

NMR imaging of density distributions in tablets

A. Djemai*, I.C. Sinka

Merck Sharp and Dohme Ltd., Hoddesdon, Hertfordshire EN11 9BU, UK

Received 12 January 2006; received in revised form 23 January 2006; accepted 27 March 2006
Available online 18 April 2006

Abstract

This paper describes the use of ^{1}H nuclear magnetic resonance (NMR) for 3D mapping of the relative density distribution in pharmaceutical tablets manufactured under controlled conditions. The tablets are impregnated with a compatible liquid. The technique involves imaging of the presence of liquid which occupies the open pore space. The method does not require special calibration as the signal is directly proportional to the porosity for the imaging conditions used. The NMR imaging method is validated using uniform density flat faced tablets and also by direct comparison with X-ray computed tomography. The results illustrate (1) the effect of die wall friction on density distribution by compressing round, curved faced tablets using clean and pre-lubricated tooling, (2) the evolution of density distribution during compaction for both clean and pre-lubricated die wall conditions, by imaging tablets compressed to different compaction forces, and (3) the effect of tablet image on density distribution by compressing two complex shape tablets in identical dies to the same average density using punches with different geometries.

Keywords: NMR imaging; Tablet; Compaction; Density distribution; Die wall friction

1. Introduction

Die compaction is a unit operation employed in pharmaceuticals, powder metallurgy, ceramics and other industries. During compaction complex movement takes place within the powder bed and interactions occur between the powder and tooling, i.e. die wall and punch faces. As a result distinct density patterns develop in the volume of the compact due to the combined effect of the main contributing factors (Sinka et al., 2003) such as: compaction behaviour of powder, friction between powder and die wall and powder and punches, geometry of die and punches, sequence of punch motion, and initial conditions of the powder before compaction, which relate to the state of the powder in the die after filling. The density distribution in tablets is important because it affects the local material properties, which in turn can influence the bioavailability of the drug and the mechanical properties of the tablets.

Density measurements in powder compacts have been carried out since the early 1900s as reviewed by Train (1957) and include techniques based on differential machining, hardness tests or X-ray shadow of lead grids placed in the compact. Macleod and Marshall (1977) have presented autoradiography experiments using ceramic compacts possessing natural radioactivity and the density distribution patterns were discussed in the context of die wall friction. Various experimental procedures have been used for characterising the density distribution in compacts made of a wide range of powders, including pharmaceutical materials (Hersey and Train, 1960; Kandeil and De Malherbe, 1977; Sixsmith and McCluskey, 1981; Charlton and Newton, 1985; Ozkan and Briscoe, 1996; Sinka et al., 2003; Eiliazadeh et al., 2004). More modern techniques available to characterise compact microstructure were reviewed by Lannutti (1997) and include X-ray CT which was also applied to characterise density distributions (Sinka et al., 2004) and defects (Wu et al., 2005) in pharmaceutical tablets.

Nuclear magnetic resonance imaging has been applied to characterise the internal structure of various materials, such as: ceramic samples, composite materials, extruded gel pastes, and tablets (Ellingson et al., 1987, 1989; Götz et al., 2002; Mantle et al., 2004; Nebgen et al., 1995).

The objective of this paper is to present the NMRI method for generating quantitative relative density maps for pharmaceutical tablets and examine the effect of tablet geometry and die wall friction on the relative density distribution at various

* Corresponding author. Tel.: +44 1992 452630; fax: +44 1992 460078.
E-mail address: abdenour_djemai@merck.com (A. Djemai).

0378-5173/$ – see front matter © 2006 Elsevier B.V. All rights reserved.
doi:10.1016/j.ijpharm.2006.03.049

stages during compaction. The relative density is defined as RD = $1 - \phi$ where ϕ represents the porosity.

2. NMR imaging method

NMR imaging is an inspection technique which provides cross-sectional images in planes through a component. The theory of nuclear magnetic resonance is well documented in texts on the subject (Callaghan, 1991) and is summarised as follows. Nuclear magnetic resonance occurs when nuclei possessing a magnetic moment μ are placed in an external magnetic field B_0, and irradiated with radio-frequency (RF) radiation B_1 perpendicular to B_0. Nuclei having a magnetic moment also possesses 'spin', a form of angular momentum characterised by the spin quantum I which for the hydrogen nucleus is equal to 1/2. When a sample containing nuclei with a magnetic moment is placed in a static magnetic field B_0 (pointing along the laboratory z-axis), the nuclear moments populate themselves between two distinct energy levels. The population difference between these two levels is governed by the Boltzmann distribution (Harris, 1986) and gives rise to a net magnetisation vector $\mathbf{M}_0 = (\mathbf{i}M_x, \mathbf{j}M_y, \mathbf{k}M_z)$. Transitions between these two energy levels may then be induced by irradiating the system with electromagnetic irradiation whose frequency is proportional to the difference of the energy level spacing:

$$\Delta E = \gamma h B_0 = h\omega_0 \tag{1}$$

where γ is the gyromagnetic ratio for ^{1}H, h is Planck's constant and ω_0 is known as the Larmor frequency. In modern NMR spectroscopy and imaging a pulse of electromagnetic radiation in the RF region is used to perturb the distribution of spins between the two energy levels. After the pulse, an RF NMR signal is detected as the equilibrium distribution between the two levels is restored. The time dependence of the signal is then monitored from which a frequency spectrum is obtained via Fourier transformation. A single sharp line in the frequency domain results if the sample contains a single proton chemical species, e.g. water. Key parameters with this technique are the spin–lattice relaxation time T_1, the spin–spin relaxation time T_2 of the sample, and the strength of the magnetic field gradient B_0, determining the image resolution, contrast, and measuring period.

NMR relaxation time has an important effect on the imaging process. T_1 is the characteristic time for the build-up of magnetic polarization of a nucleus, and directly affects the rate at which data can be accumulated from successive acquisitions of NMR signals during the production of an image. It therefore controls the total time to acquire an image and the signal-to-noise (S/N) ratio achieved per unit time. T_2 is the characteristic time for the decay of the transverse precessing magnetic moment which is detected as the NMR signal. T_2 affects the achievable spatial resolution and S/N ratio. Long T_2s are desirable, and are found in compounds which have minimal spin–spin coupling and which form non-viscous solutions. T_2 should be significantly greater than the echo time TE in order to avoid limiting spatial resolution and S/N ratio.

3. Materials and tablet preparation

3.1. Tablet compression

The tablets were compressed using a press where the bottom punch was stationary with respect to the die. Round and capsule shaped tablets were manufactured from microcrystalline cellulose (grade Avicel PH102, manufactured by FMC BioPolymer, Cork, Ireland). The nominal mean particle size of the powder is 100 μm and the full density of the material is 1520 kg m^{-3}. The bulk density of the powder is around 300 kg m^{-3}.

The characteristics of the round tablets are presented in Table 1. The tablets were compressed using curved faced tooling having a cup radius of 8.03 mm, which is commonly referred to as deep concave tooling. In order to generate snapshots of density distributions at various stages of compaction, series of tablets were compacted to different compaction forces.

The effect of friction between powder and tooling was examined by compressing tablets using clean and pre-lubricated tooling as follows:

- In order to achieve high friction between powder and tooling the die and punches were degreased prior to compaction: this is referred to as "clean" tool condition.
- In order to achieve low friction the die and punches were preconditioned by compressing pure magnesium stearate (a common pharmaceutical powder lubricant): this is referred to as "lubricated" tool condition.

In order to study the effect of geometry for complex shape tablets, two tablets were compressed in identical dies using tooling with different cup geometries. The top surfaces of the tablets had different break-lines while on the lower surfaces the letters

Table 1
Characteristics of round tablets

Tablet	m (g)	D (mm)	H (mm)	Compression force (N)	RD	Condition
NMR_01	0.314	8.78	9.11	500	0.435	Clean
NMR_02	0.324	8.78	7.88	1000	0.533	Clean
NMR_03	0.320	8.76	6.59	2000	0.655	Clean
NMR_04	0.320	8.76	6.08	3000	0.724	Clean
NMR_05	0.320	8.77	7.68	1000	0.543	Lubricated
NMR_06	0.327	8.76	6.01	3000	0.751	Lubricated
NMR_07	0.335	8.74	5.59	4950	0.845	Lubricated

Table 2
Characteristics of capsule shape tablets

Tablet	Thickness (mm)	Weight (g)	Total volume (mm^3)	Average density ($kg\,m^{-3}$)	Compression force (N)
NMR_08	3.90	0.190	159.72	1189	4000
NMR_09	4.19	0.175	143.25	1221	3500

"MSD" were embossed. The characteristics of these tablets are presented in Table 2. The tablets were prepared to similar average relative densities using tools in clean condition. The density distribution in these tablets was characterised using X-ray CT and the results were published elsewhere (Sinka et al., 2004). By performing NMRI imaging on the same tablets it was possible to compare the results from both techniques, as discussed in Section 5.3.

In addition, round, flat-faced disks were also produced in order to perform validation experiments, which are also presented in Section 5.3. The requirement for these compacts is that they have uniform density. For round flat geometry the density gradients are induced due to the effect of friction between powder and die wall. In the absence of friction between powder and die wall round, flat faced tablets are uniform. Therefore, in order to minimise the effect of friction the tools were used in lubricated condition. The characteristics of the flat faced tablets are given in Table 3.

3.2. Oil immersion

To image the internal porosity of the tablets, a filler fluid that gives a good NMR signal is used as a marker to contrast with the low signal intensity of a solid body. The fluid is introduced into the test samples by vacuum impregnation. The amount of fluid locally present within the tablet is then determined by ^{1}H NMR imaging, revealing the inverse inner structure by displaying the porosity distribution. The high signal intensity regions correspond to regions of high porosity. It is assumed that the porosity is connected and that the fluid fully impregnates the pore space. Uneven porosity distributions within tablets as well as cracks and cavities can also be visualised with this method. The filler fluid approach provides a means to visualize internal volumes that are larger than the spatial resolution of the measurement, which is about 40 μm within the image plane for the measurements presented here. Volumes smaller than the resolution (specifically, the microscopic volumes that constitute the pore structure) are not resolved. The fractional porosity is the fractional image intensity (i.e., image intensity normalized to the intensity of pure filler fluid).

Table 3
Characteristics of disks used for method validation

Tablet	*m* (g)	*H* (mm)	*D* (mm)	Compression force (N)	RD
Ref 01	0.099	2.03	8.76	1000	0.533
Ref 02	0.121	2.00	8.74	2000	0.661
Ref 03	0.141	2.08	8.75	3000	0.738
Ref 04	0.155	2.03	8.74	4900	0.837

Desirable chemical properties of the filler fluid include a high concentration of the observed nuclear isotope and chemical compatibility with the sample (no chemical reaction, dissolution, or swelling). In this study we employed a highly refined mineral oil (Bayol 82, manufactured by ExxonMobil Lubricants & Specialities), which was found compatible with microcrystalline cellulose. By measuring the oil uptake for the tablets considered it was concluded that more than 95% of the porosity was filled with oil, suggesting that the above assumption was acceptable.

4. NMR parameters

Desirable NMR properties of the filler fluid include the presence of a high-sensitivity isotope. Hydrogen protons are the best choice; the isotope with the next highest sensitivity is ^{19}F, with an intrinsic sensitivity 0.8 that of ^{1}H. To avoid artefacts and anomalous signal intensity variations, the filler fluid must exhibit a simple NMR spectrum, ideally containing a single sharp resonance line. Such a simple spectrum results from the absence of chemical shift differences and spin–spin (or *J*) couplings within the molecule, and will be exhibited by a compound possessing a high degree of chemical symmetry (i.e., chemical and magnetic equivalence of nuclei). The MRI experiments were performed on a Bruker DRX 400 MHz spectrometer operating at a ^{1}H frequency of 400.13 MHz. A single tuned 10 mm, ^{1}H, saddle coil RF insert was used to excite the sample in combination with a MICRO5 imaging probe. Spatial resolution was achieved using a three-axis actively shielded gradient system capable of producing a magnetic field gradient of 200 G/cm in all three Cartesian directions. A standard spin echo (SE) pulse sequence was used. The solid substance of tablets could not directly be visualised with this spin echo method. This is because NMR signals for most solids typically show broadened linewidth and cannot be evaluated for imaging using the standard spin echo pulse sequence due to an extremely low intensity of the image signal caused by the very short T_2 relaxation time. A short TE of 4 ms was used to minimize signal intensity loss due to diffusion of the oil molecules through the interfacial field gradients that exist at the magnetic susceptibility discontinuities of the sample. The pulse repetition time, TR, was approximately 2 s. The digital resolution in the images was 256 pixels by 256 pixels, corresponding to pixel sizes of 40 μm. The slice thickness (depth of the sample voxel) was 0.5 mm. The test samples typically span the order of 100 pixels in these images. We determined that under our imaging conditions the tablet material did not give any significant NMR signal. Typical imaging times were approximately 1 h corresponding to 16 signal averages per phase-encoding gradient step. We measured signal intensities over regions of interest and calculated the averages directly from the stored NMR data.

The samples were examined in 10 mm glass test tubes inserted into the 10 mm coil. In order to fix the tablets inside the test tubes, a sample holder built of Teflon was used. The maximum simultaneously imaged height was ca. 12 mm. The smallest examined volume unit, defined as voxel, was $(40\ \mu m)^3$. The measured NMR signal homogeneity obtained was reasonably good across the examined image areas. Consequently, for the images of the microcrystalline cellulose tablets the correction for coil signal inhomogeneity was considered unnecessary.

5. Results and discussion

Before presenting experimental relative density maps it is instructive to summarise the main factors contributing to the development of density distributions in tablets (Sinka et al., 2003) which are:

- The behaviour of powder during compaction, which encompasses particle interaction, deformations, fracturing, interparticulate friction, rate effects etc., which can be described using appropriate constitutive models.
- The friction interaction between powder and tooling, which can be described by a friction coefficient.
- Geometry of the problem, i.e. the shape of die and tooling.
- Pressing sequence, i.e. the relative motion of die and punches.
- Initial conditions, which relate to the condition of the powder after die fill. In this study the die was filled by hand with awareness to create a uniform initial state.

The final density distribution in a tablet is a result of the combined contribution of the above factors. The consequence of low and high-density regions is that the local properties of the powders are affected. The strength of a porous material generally increases with density. From this point of view, the importance of such low-density regions is that they may affect picking and sticking and are prone to surface erosion, abrasion or breaking during post-compaction operations such as transport, coating or packaging. In addition, the disintegration and dissolution behaviour may be affected.

5.1. Effect of friction between powder and tooling

In this section we examine the density distributions in various cross-sections of tablets manufactured using both lubricated and clean tooling as presented in Table 1. The relative density maps are presented in Fig. 1. Both sets of tablets (clean and lubricated tool conditions) present high-density regions particularly at the edge which extends around the entire tablet periphery. A comparison between two tablets compressed to the same compaction force of 3000 N is detailed as follows. For the tablet compressed in a clean die the density reaches 1200–1300 kg m^{-3} locally in some areas as shown in Fig. 1d (NMRI_04-D6) versus 1100–1200 kg m^{-3} for tablets compressed with the same force in a lubricated die as shown in Fig. 1f (NMRI_6-D6). However the average density of the tablet compressed using lubricated tooling is higher that for clean tooling. Other regions, such as the top (D12) and bottom (D13) centre of the tablet present densities of 900–1000 kg m^{-3} when using a clean die versus 1000–1100 kg m^{-3} when using a lubricated die. For both sets of tablets the RD at the top corner of specimen is higher than at the bottom.

For the clean tool condition as a result of the high coefficient of friction between powder and die wall (and powder and punches) there is little or no movement of powder with respect to the punch face as the top punch makes progressive contact with the surface of the powder during compaction. Consequently regions around the band area, where the powder undergoes larger vertical strains, become denser than those in the cup area, these effects are evident in Fig. 1a–d.

If powder sliding with respect to the punch face is allowed (i.e. lubricated tool condition), then the high density areas form an X-shaped pattern as illustrated in Fig. 1e–g.

In all cases a lower density region is observed at the top centre of the tablet. This is attributed to the top punch making contact with this area at a later stage during compaction. Around the vertical axes, however, the tablets are symmetrical as expected.

5.2. Effect of tablet geometry

The geometry of the capsule shape tablets NMR_08 and NMR_09 described in Table 2 is illustrated in Fig. 2 also indicating a reference system for the orthogonal cross sections of the density distribution maps which are presented in Fig. 3. The vertical *Y–Z* cross-sections at the centres of the tablets are presented in Fig. 3a, d and the horizontal *X–Z* cross-sections through the mid-height of the tablets are presented in Fig. 3c, f. Tablet NMR_08 presents high-density regions under the break-line and in the band area—particularly at the edge, as shown in Fig. 3a. The two very high-density spots in Fig. 3c correspond to the positions where the break-line, which is curved around the face of the punch, is at closest with respect to the bottom of the tablet. The density pattern below the break-line may affect the ability to effectively break the tablet in half. Similar observations can be made for tablet NMR_09 as illustrated in Fig. 3d and f. The density gradients around the band area are amplified by the particular geometry of the cup. The regions of lower density at the top of the cup (to the sides of the break-line) and at the bottom of the cup (where the characters are embossed) are more extensive, while the high density areas become more localised. The high-density regions around the band area are diminished and there is little evidence of dense regions below the break-line.

Fig. 3b and e presents *X–Y* cross-sections (parallel to the break-line). It is interesting to note that the capsule shape tablets are not symmetrical with respect to a horizontal plane through the middle (i.e. the density around the band area at the top of the tablet is larger than at the bottom). There are two main causes for this effect. First that the geometry of the powder bed is asymmetrical prior to the compaction, because the bottom punch is filled with powder while the top punch cavity is empty. Second, the sequence of punch motions employed: the bottom punch was maintained stationary with respect to the die. The high friction coefficient between powder and die wall results in higher density at the top as the top punch is displaced downwards forming the tablet. This is consistent with the observations for round tablets

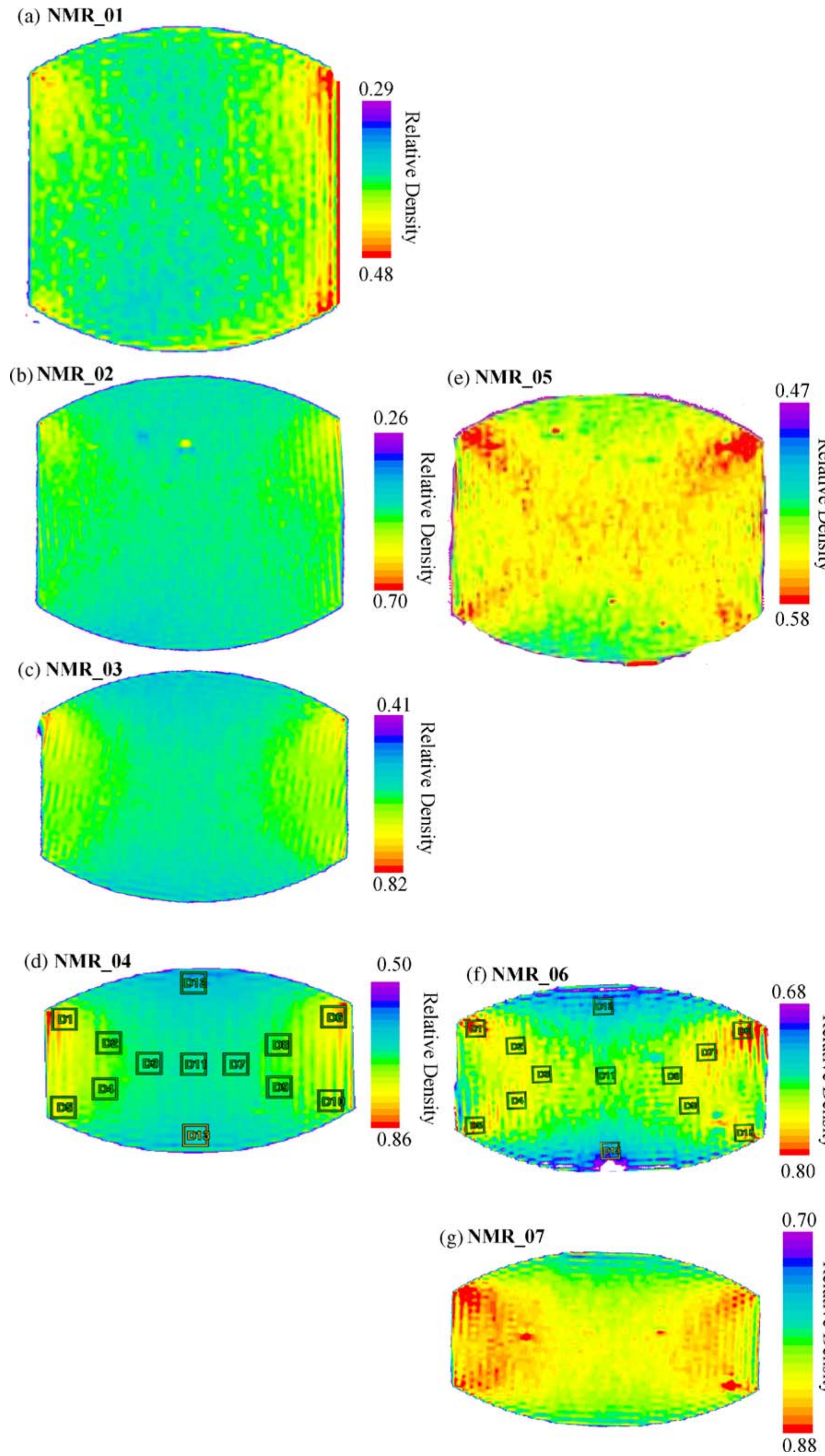

Fig. 1. Relative density maps (vertical cross-section) for tablets compacted in a unlubricated die (a)–(d) and lubricated die (e)–(g). (a) NMRI 01, (b) NMRI 02, (c) NMRI 03, and (d) NMRI 04. For (d) D1 = 0.79, D2 = 0.73, D3 = 0.70, D4 = 0.73, D5 = 0.77, D6 = 0.81, D7 = 0.70, D8 = 0.72, D9 = 0.72, D10 = 0.75, D11 = 0.69, D12 = 0.64, and D13 = 0.66. (e) NMRI 05, (f) NMRI 06, and (g) NMRI 07. For (f) D1 = 0.78, D2 = 0.76, D3 = 0.76, D4 = 0.76, D5 = 0.77, D6 = 0.78, D7 = 0.77, D8 = 0.75, D9 = 0.76, D10 = 0.77, D11 = 0.74, D12 = 0.71, and D13 = 0.70.

compressed in clean tooling presented in Fig. 1. However, the results cannot be generalised. Even for an axisymmetric (round) tablet the powder movement is complex in both axial and radial direction during compaction.

5.3. Method validation

The relative density distribution in vertical cross-sections of the uniform flat disks described in Table 3 is presented in Fig. 4.

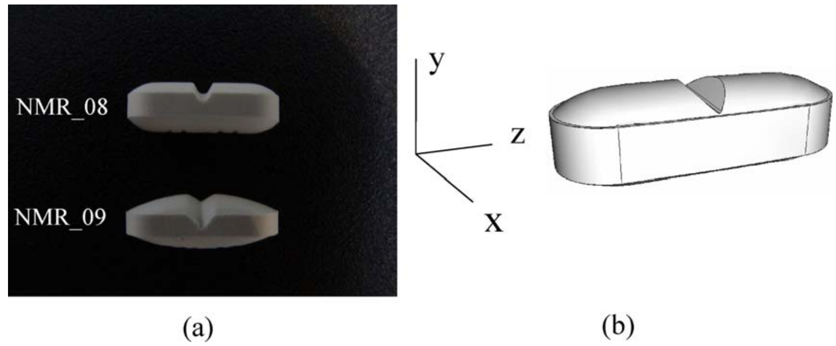

Fig. 2. Capsule shaped tablets: (a) geometry and (b) reference axes.

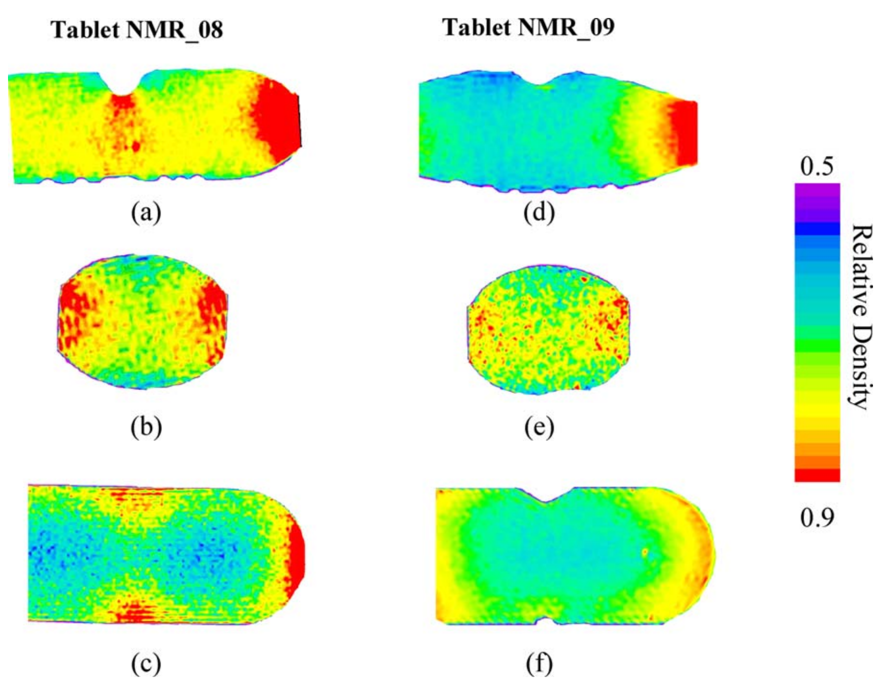

Fig. 3. Relative density maps in *Y–Z* cross-sections (a and d), *X–Y* cross-sections (b and e), and *X–Z* cross-sections (c and f).

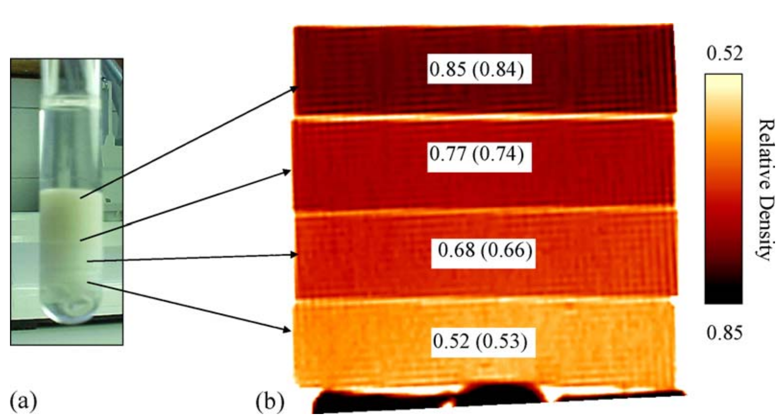

Fig. 4. Validation of NMRI technique using uniform flat disks. The theoretical RD (from weight and dimension measurements) is indicated in brackets. (a) Image of the stacked flat disks in the NMR tube and (b) NMR images of a vertical cross-sections.

Table 4
Summary of comparison between X-ray and NMRI results: average density difference (with respect to NMRI results)

	Tablet NMR-08		Tablet NMR-09	
	Section *YZ*	Section *XZ*	Section *YZ*	Section *XZ*
Average (%)	7.15	3.86	6.19	2.86
Minimum (%)	2.93	0.72	2.82	0.43
Maximum (%)	11.84	7.31	10.96	5.81

The agreement between the calculated and measured average RD is good. These results validate the NMR imaging technique for characterising density distributions.

As described in Section 3.1 the same capsule shaped tablets have been characterised previously using X-ray CT (Sinka et al., 2004) to allow direct comparison between the methods. Similar to Fig. 1d and f, 17 square areas having a size of approximately 5 mm × 5 mm were selected from *XY* and *XZ* cross-sections to cover both high- and low-density areas. The density was averaged in each region, and then these were averaged for the entire cross-section. The data between X-ray CT and NMRI were compared. The difference was expressed as percent with respect to the NMR results as presented in Table 4. Overall there is a good agreement between the two methods. The density indicated by the NMRI data was found to be slightly higher than the X-ray CT data in a consistent manner. Although we attempted to make like-for-like comparisons, the following issues should be considered when interpreting the differences:

- The sections compared are not identical. For example, section *YZ* in Fig. 3 was chosen to be approximately in the middle of the tablet but the positioning is not exact. A corresponding section was chosen for the X-ray data, this is not positioned exactly either.
- The areas were first selected on the NMRI data. The corresponding areas for the X-ray data were selected so that they are approximately in the same locations, but there is no perfect one to one correspondence.
- The sizes of the selected areas (approximately 5 mm × 5 mm) may not be identical.

Table 4 illustrates that the average differences for the two tablets are 7.15% and 6.19% for the *YZ* sections. These values are considerably higher that the average differences for the *XZ* sections, 3.86% and 2.86%. This can be attributed partly to the fact that *YZ* sections have the largest gradients and therefore are more sensitive to the issues highlighted above. Based on the above consideration, however, it can be concluded that carefully conducted experiments can generate accurate results.

6. Conclusions

NMR imaging was applied to examine the density variation in pharmaceutical tablets. Quantitative density maps were generated without applying corrections to the NMR data. The method was validated by using reference disks and also by comparison with X-ray CT.

The effect of geometry and friction between powder and tooling was evaluated systematically for simple and complex shaped tablets at various stages of compaction. Tablets present complex density distributions as a combined contribution from various factors. Each tablet is unique in terms of the compaction behaviour of the material, friction between powder and tooling, geometry, pressing sequence and initial conditions that result from die fill. By understanding each of these elements and their combined interaction it is possible to engineer a tablet microstructure that gives improved mechanical and drug bioavailability behaviour.

Acknowledgements

Special thanks to Drs. Steve Burch and James Tweed, AEA Technology Ltd. for making comparison with X-ray CT data possible; this work was conducted as part of project MPM5.2 funded by the Department of Trade and Industry, UK. The management of PR&D, particularly Drs. D.E. Storey and S.D. Reynolds, of Merck Research Laboratories are gratefully acknowledged for their support.

References

Callaghan, P.T., 1991. Principles of Nuclear Magnetic Resonance Microscopy. Oxford University Press, Oxford.

Charlton, B.J., Newton, M., 1985. Application of gamma-ray attenuation to the determination of density distributions within compacted powders. Powder Technol. 41, 123–134.

Eiliazadeh, B., Pitt, K., Briscoe, B., 2004. Effects of punch geometry on powder movement during pharmaceutical tabletting processes. Int. J. Solids Struct. 41, 5967–5977.

Ellingson, W.A., Ackerman, J.L., Garrido, L., Weyand, J.D., Dimilia, R.A., 1987. Characterisation of porosity in green-state and partially densified Al_2O_3 by nuclear magnetic resonance imaging. Ceram. Eng. Sci. Proc. 8, 503–512.

Ellingson, W.A., Wong, P.S., Dieckman, S.L., 1989. Magnetic resonance imaging: a new characterisation technique for advanced ceramics. Ceram. Bull. 68, 1180–1186.

Götz, J., Eisenreich, N., Geißler, A., Geißler, E., 2002. Characterisation of the structure in highly filled composite materials by means of MRI. Propell. Explos. Pyrot. 27, 179–184.

Harris, R.K., 1986. Nuclear Magnetic Resonance Spectroscopy. Longman.

Hersey, J.A., Train, D., 1960. Powder Metall. 6, 20–35.

Kandeil, A., De Malherbe, M.C., 1977. The use of hardness in the study of compaction behaviour and die loading. Powder Technol. 17, 253–257.

Lannutti, J.J., 1997. Characterisation and control of compact microstructure. MRS Bull. 22, 38–44.

Macleod, H.M., Marshall, K., 1977. The determination of density distributions in ceramic compacts using autoradiography. Powder Technol. 16, 107–122.

Mantle, M.D., Bardsley, M.H., Gladden, L.F., Bridgwater, J., 2004. Laminations in ceramic forming—mechanisms revealed by MRI. Acta Mater. 52, 899–909.

Nebgen, G., Gross, D., Lehmann, V., Müller, F., 1995. ^{1}H NMR microscopy of tablets. J. Pharm. Sci. 84, 283–291.

Ozkan, N.B., Briscoe, J., 1996. The surface topography of compacted agglomerates; a means to optimise compaction conditions. Powder Technol. 86, 201–207.

Sinka, I.C., Cunningham, J.C., Zavaliangos, A., 2003. The effect of wall friction in the compaction of pharmaceutical tablets with curved faces: a validation study of the Drucker-Prager Cap model. Powder Technol. 133, 33–43.

Sinka, I.C., Burch, S.F., Tweed, J.H., Cunningham, J.C., 2004. Measurement of density variations in tablets using X-ray computed tomography. Int. J. Pharm. 271, 215–224.

Sixsmith, D., McCluskey, D., 1981. The effect of punch tip geometry on powder movement during the tabletting process. J. Pharm. Pharmacol. 33, 79–81.

Train, D., 1957. Transmission of forces through a powder mass during the process of pelleting. Trans. Inst. Chem. Eng. 35, 258–266.

Wu, C.-Y., Ruddy, O.M., Bentham, A.C., Hancock, B.C., Best, S.M., Elliott, J.A., 2005. Modelling the mechanical behaviour of pharmaceutical powders during compaction. Powder Technol. 152, 107–117.